**10A.1**

# THE ROLE OF DEEP CONVECTION IN MOISTENING THE INNER CORE REGIONS OF DEVELOPING TROPICAL CYCLONES: EVIDENCE FROM GRIP 2010

Jonathan Zawislak* and Ed Zipser
University of Utah, Salt Lake City, Utah

## 1. INTRODUCTION

The 2010 NASA Genesis and Rapid Intensification Processes (GRIP) campaign (Braun et al. 2012), conducted concurrently with the NSF/NCAR Pre-Depression Investigation of Cloud Systems in the Tropics (PREDICT; Montgomery et al. 2012) and NOAA Intensity Forecast Experiment (IFEX), provides an unprecedented high spatial and temporal resolution dataset of tropical cyclogenesis events. In-situ data from coincident and consecutive flights into developing Karl and Matthew, combined with conventional geostationary IR and overpasses of passive microwave (PMW) instruments, offers the best opportunity to date to examine, in detail, the pre-genesis wind field at multiple levels, deep convection, and the time evolution of the thermodynamic properties of the developing inner core. The goal of this paper is to describe the relationship between deep convective episodes in pre-Karl and the thermodynamic characteristics of the inner core, as well as offer insight into what ultimately determines the fate of disturbances with apparent genesis potential.

## 2. DATA AND METHODOLOGY

For each disturbance, the "center" is defined by the vorticity maximum (VM) manually tracked in the 1°x1° NCEP FNL model analyses. Although 925, 700 and 600 hPa VMs are also tracked, the analyses presented in this paper are based on the 850 hPa VM center. The inner core is defined as the region within 3° of the VM center. Dropsonde data from PREDICT-GRIP-IFEX (PGI) and USAF C-130s are interpolated to 17 pressure levels and combined into a single dataset, which is then composited to describe the thermodynamic evolution of the inner core (Section 3). To describe convective characteristics, hourly IR information is combined with PMW data, when available (Section 4). PMW platforms included in the analysis are TRMM TMI, AMSR-E, and SSM-I(S) 15, 16, and 17; these instruments offer brightness temperature ($T_b$) and derived total precipitable water (TPW; from REMSS, online at http://www.ssmi.com). Likewise, AIRS TPW and RH information is also available for analysis. For rainfall, TRMM 3B42 (merged IR) data is available 3-hourly at 0.25°.

Given that not all swaths from PMW platforms completely cover the inner core, the fractional coverage of data within 3° is computed for each swath. To be considered for the analysis, the swath must contain data within 0.5° of the VM center; this ensures that for most overpasses included, the fractional coverage of data within the inner core is at least 40%. For AIRS, the fractional coverage may be lower since data in raining areas must be excluded.

## 3. THERMODYNAMIC EVOLUTION OF PGI GENESIS CASES FROM DROPSONDES

Figure 1 shows the composite equivalent potential temperature ($\theta_e$) anomaly for all genesis cases investigated by the PGI campaigns during 2010. All PGI and USAF dropsondes are included, totaling 668 before and 1539 after genesis. Data is composited in 1-day periods for 4 days before and after formation (defined as TD classification by the NHC). The anomaly is defined by the difference between the mean profile of the inner core dropsondes for each 1-day period, and the mean profile of environmental (between 3° and 7° of the VM center) soundings from all PGI flight days. Figure 1 illustrates an important characteristic of developing tropical cyclones; their mean mid level $\theta_e$ is higher than that of the surrounding environment and will increase slightly each day, while the low-levels exhibit little increase until after formation.

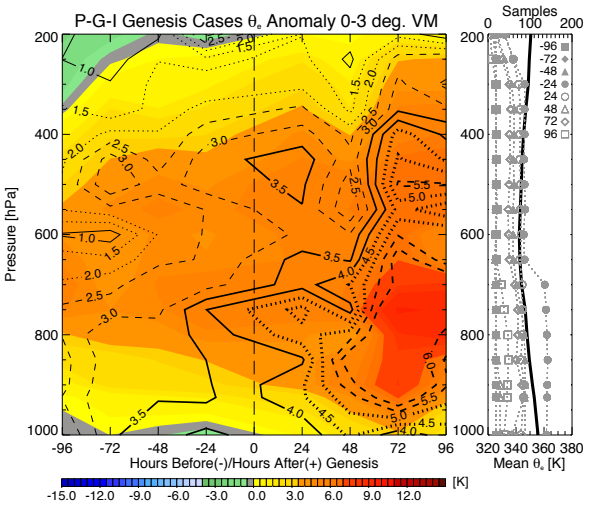


Figure 1: Composite $\theta_e$ anomaly (color shaded) of all dropsondes within 3º of the 850 hPa VM center for all PGI genesis cases; black contours are standard deviation.

* *Corresponding author address:* Jonathan Zawislak, Univ. of Utah, Dept. of Atmos. Sci., 135 South 1460 East, Salt Lake City, UT 84112; email: jon.zawislak@utah.edu

Figure 2 similarly illustrates the time evolution of the potential temperature (θ) and indicates that the warm core is developing at mid to upper levels (above 600 hPa) as many as 3 days before genesis. However, given the relatively small magnitude of the θ anomaly compared to $\theta_e$, the positive, increasing (albeit slowly) $\theta_e$ anomaly at mid levels is attributed to an increase in moisture content. Likewise, another important observation from Figure 2 is the persistent cool anomaly at low-levels.

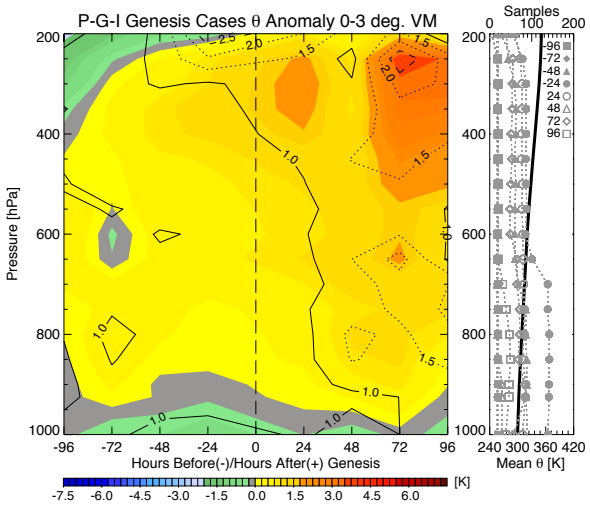


Figure 2: Composite θ (color shaded) of all dropsondes for PGI genesis cases; black contours are standard deviation.

## 4. TIME EVOLUTION OF PRE-KARL CONVECTION

Karl was classified a tropical depression at 1200 UTC on 14 September near 82ºW, 17.5ºN. Seventeen total flights by dropsonde-equipped PGI and USAF aircraft investigated Karl in the 5 days up to, and including, formation. The evolution of the low level (925 hPa) and mid level (600 hPa) wind field from dropsondes is shown in Figure 3. This figure indicates that the low and mid level circulation only became organized late on 13 September; prior to this day, the wave exhibited a SW-NE horizontal tilt, in which the southeasterly winds on the east side of the trough axis were stronger than the northeasterly winds on the west side. We hypothesize that only when the winds became more symmetric on 13 September did the wave vorticity come predominately from curvature, rather than from shear, and thus more favorable for formation.

Figure 4 shows the time evolution of IR cloud fraction. This figure indicates that Karl's convection exhibits a distinct diurnal cycle before formation, and convection only persists through the diurnal cycle after reaching TS intensity. In fact, as may be surmised in both Figures 4 and 5 (similar to Figure 4, except for rain rate), the most widespread, intense convective episode occurs *3 days* before genesis. Each subsequent convective episode, although still intense, has less areal coverage and is farther from the VM center. The inner core statistics are consistent with these results as the time series of raining fraction and convective raining fraction (Figure 6b) indicates a decrease in areal coverage in each episode in the 3 days leading up to formation.

To further characterize the intensity of each convective episode, $T_b$ (henceforth, polarized corrected temperature; PCT) statistics from TMI (85 GHz), AMSR-E (89 GHz), and SSM-I/S (85/91 GHz) overpasses of the VM are computed (Figure 6c). These higher frequency channels are sensitive to precipitation-sized ice particles, and thus are more reliable indicators for convective intensity than conventional IR (Spencer el al. 1989). According to the minimum and mean PCT (for pixels ≤ 250 K), no convective event is noticeably more intense than any other prior to formation. In fact, the final convective episode before formation (around 1800 UTC on 13 September) is characteristically the *least* intense; the fractional coverage of pixels ≤ 250 K is nearly 10% less, and minimum PCT as much as 40 K warmer, than previous episodes.

Synthesizing the information given by the dropsondes, IR, and PMW overpasses, we now attempt to identify a relationship between deep convective episodes and moisture content of pre-Karl's inner core. Figure 6d shows the derived TPW from AMSR-E, TMI, SSM-I(S) and AIRS, as well as the median TPW computed from dropsondes for each DC-8 and G-V flight. For inclusion, the minimum pressure level available in the dropsonde data is required to be 400 hPa, while the maximum, 975 hPa. Also shown in Figure 6d is the 400-750 hPa (mid level) layer average water vapor mixing ratio from dropsondes, and for comparison, NCEP FNL model analysis.

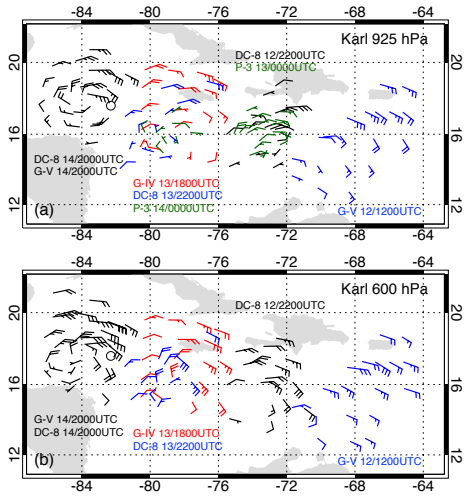


Figure 3: Select dropsonde observations of Karl from 12-14 September. Flights are separated by color and dropsonde locations are time-space adjusted, based on the zonal phase speed of Karl, to the time indicated.

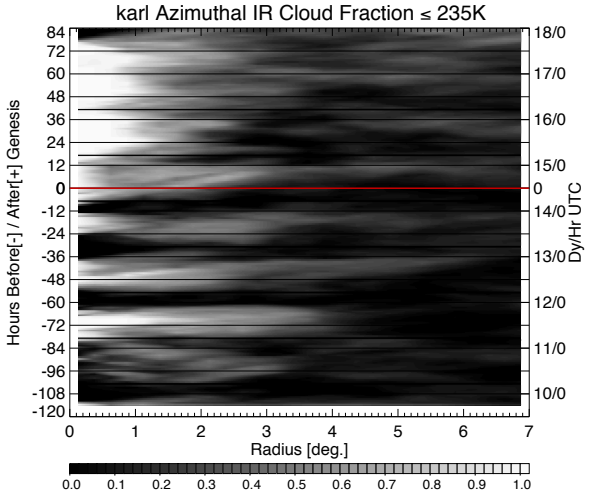


Figure 4: IR cloud fraction for $T_b \leq 235$ K as a function of radial distance from the 850 hPa VM center.

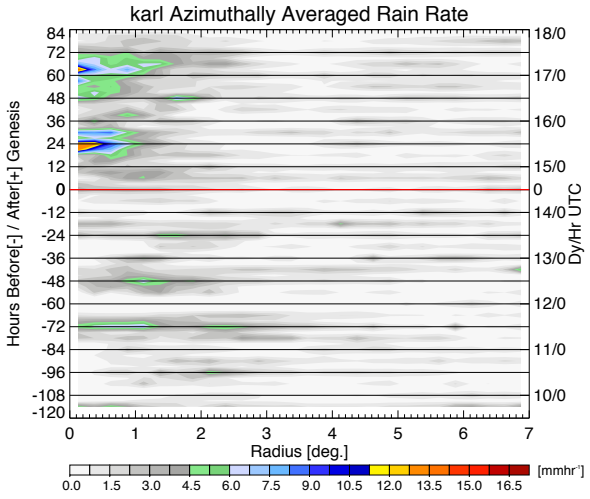


Figure 5: Average rain rate (from TRMM 3B42) as a function of radial distance from the 850 hPa VM center.

Figure 6d indicates that after an initial increase (~4 kg $m^{-2}$) in TPW on 10 September, the inner core exhibits only a slight increasing trend (~1-2 kg $m^{-2}$) on subsequent days. Likewise, during each minimum in the diurnal cycle, the mid level water vapor mixing ratio shows no noticeable increase from the previous minimum. Once the TPW of pre-Karl's inner core exceeds 55 kg $m^{-2}$, deep convection apparently does little to further moisten the inner core. These results, therefore, indicate that the inner core of pre-Karl is thermodynamically primed for formation well before the actual "genesis" time.

## 5. SUMMARY AND CONCLUSIONS

The time evolution of inner core convective and thermodynamic properties from developing disturbances during the summer of 2010 have been investigated using the unprecedented dropsonde dataset made available by GRIP, PREDICT, IFEX and USAF aircraft, as well as, conventional IR and numerous PMW overpasses. After a careful synthesis of dropsonde and satellite observations, a case study of pre-Karl indicates that, thermodynamically, the disturbance is primed for formation well before genesis occurs. Likewise, an analysis of deep convective episodes prior to formation indicates that the most favorable episode (in terms of convective intensity, raining fraction and proximity to the center) occurred *3 days* prior to TS classification, while the convective episode just prior to classification was perhaps the *least* impressive of the pre-genesis stage. Therefore, considering the convective history, and that the inner core is already moist, the formation of Karl is more closely tied to the wave organization on 13 September, rather than to any distinguishing characteristic of the convection.

## 6. REFERENCES


Braun, S., and Co-authors, 2012: NASA's Genesis and Rapid Intensification Processes (GRIP) Field Experiment – Bringing New Technologies to the Hurricane Intensity Problem. *Bull. Amer. Meteor. Soc.*, submitted.

Montgomery, M.T., and Co-authors, 2012: The Pre-Depression Investigation of Cloud Systems in the Tropics (PREDICT) Experiment: Scientific Basis, New Analysis Tools, and Some First Results. *Bull. Amer. Meteor. Soc.*, **93**, 153-172.

Spencer, R.W., H.M. Goodman, and R.E. Hood, 1989: Precipitation retrieval over land and ocean with the SSM/I: Identification and characteristics of the scattering signal. *J. Atmos. Oceanic Technol.*, **6**, 254-273.


## 7. ACKNOWLEDGMENTS


The GRIP field program and subsequent research is under the leadership and support of Dr. Ramesh Kakar, NASA Headquarters. This research is supported by NASA grant NNX09AC44G. The authors also thank Joe Turk, Svetla Hristova-Veleva and Paola Salio for providing the IR data.

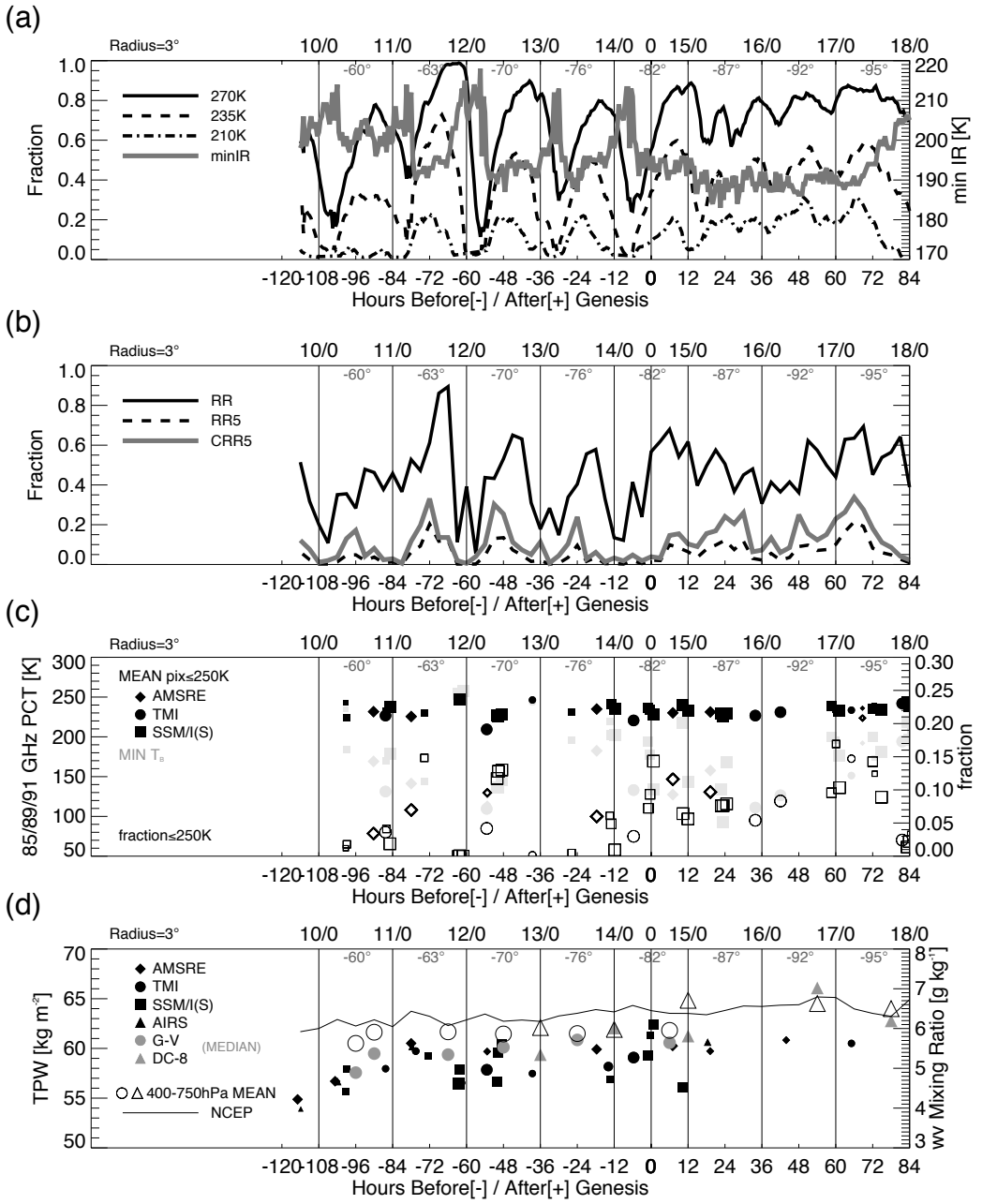


Figure 6: (a) Time series of fraction of IR pixels within 3º of 850 hPa VM center with $T_b \leq 210$ (black, solid), 235 (dash), 210 K (dash-dotted), as well as minimum IR $T_b$ (gray, solid); (b) fraction of raining pixels (solid, black) within 3º of 850 hPa VM center, fraction of total pixels within 3º with rain rate ≥ 5 mm $hr^{-1}$ (dashed), and convective fraction, i.e. the fraction of raining pixels with rain rate ≥ 5 mm $hr^{-1}$ (gray, solid); (c) mean PCT of pixels ≤ 250 K within 3º of 850 hPa VM center (filled black), minimum PCT (filled gray), and fraction of pixels within 3º that are ≤ 250 K (open symbols). (d) TPW from satellites (filled, black) and aircraft (filled, gray), 400-750 hPa mean water vapor mixing ratio from aircraft (open) and NCEP FNL (solid line).

For (c) and (d), the size of the symbol indicates the fractional coverage of data within the 3º radial circle around the 850 hPa VM center; the larger symbol, the higher the fractional data coverage in the swath.